

## Exploring structure activity relationships in the acetoxylation of small olefins

Stephan Andreas Schunk<sup>a,\*</sup>, Christian Baltes<sup>b</sup>, Andreas Sundermann<sup>a,\*</sup>

<sup>a</sup> *hte Aktiengesellschaft, Kurpfalzring 104, 69123 Heidelberg, Germany*

<sup>b</sup> *Max-Planck-Institut für Kohlenforschung, Kaiser-Wilhelm-Platz 1, 45470 Mülheim an der Ruhr, Germany*

Available online 7 July 2006

### Abstract

The diacetoxylation of butadiene in the liquid phase is part of an industrially established interesting alternative route to tetrahydrofurane (THF) competing with the currently most attractive route of butane oxidation to maleic anhydride and subsequent hydrogenation to THF. Although successfully executed in the liquid phase, no viable gas phase process has been realised for the diacetoxylation of butadiene until today. In this paper we present our results on screening campaigns focussed on Pd–K–X–Y libraries tested in a 192-fold reactor system for the acetoxylation of butadiene, butenes, propene and ethylene. An in depth analysis of the compositional space with the Pd–K–X–Y systems was conducted together with a sensitivity analysis regarding the feed constituents butadiene, acetic acid and oxygen. In the screening campaign we could identify a new catalyst system based on Pd–K–Bi–Pt which outperforms all other catalysts tested especially in the diacetoxylation of butadiene and the acetoxylation of ethylene. Based on the results obtained we also propose an alternative mechanistic pathway for the acetoxylation which proceeds via radicals as intermediates. The alternative mechanism is supported by our results obtained on quantum mechanical calculations.

© 2006 Elsevier B.V. All rights reserved.

**Keywords:** Partial oxidation; Acetoxylation; Butadiene; Tetrahydrofurane; High throughput experimentation

### 1. Introduction

The economically highly attractive and atom efficient technical route to THF via diacetoxylation of butadiene was first implemented by Mitsubishi Chemical on a production scale in 1982 with a yearly tonnage of 20,000 t [1–3]. The diacetoxylation reaction of butadiene in the current process is performed in the liquid phase employing trickle bed conditions under mild conditions with regard to the temperature of 70–150 °C and pressures of 70–150 bar with acetic acid as the solvent and an oxygen containing gas phase. The typical catalyst systems resemble partly those used for the catalytic conversion of acetic acid and ethylene to vinylacetate and are based on (supported) palladium doped with Sb, Bi, Se or Te as dopants, still they lack the typical alkali components used for gas phase catalysts. Apparently palladium is the key element for the formation of esters from acetic acid and olefins, yet

without doping of Sb, Bi, Se or Te no substantial amounts of the acetoxylation and diacetoxylation product are formed [2]. Comparing the chemistry involved for this process with the process for the production of vinylacetate from ethylene and acetic acid it becomes evident that it in principle should also be possible to perform the diacetoxylation of butadiene in the gas phase. Although the gas phase acetoxylation of butadiene has not yet reached the stage of an established chemical process, stimulating results were obtained from several groups [4–6]. The typical challenges that are reported are that mainly the mono-acetoxylation product is obtained and high selectivities to products of value can only be obtained at low conversions up to 5%, with selectivities dropping sharply beyond that threshold [7–11]. This was an incentive for us to look for catalyst systems and process conditions that would give new insight in the gas phase diacetoxylation by (a) systematically investigating the traditional and new compositions and dopants over a wide compositional range and (b) a broad variation for the feed parameters employed. For the high throughput screening we employed a Stage I system in which 192 catalysts can be evaluated in parallel via infrared thermography and GC–MS analysis (see Fig. 1) [12]. Apart from the sequential screening

\* Corresponding authors.

E-mail address: [stephan.schunk@hte-company.de](mailto:stephan.schunk@hte-company.de) (S.A. Schunk).

URL: <http://www.hte-company.de>

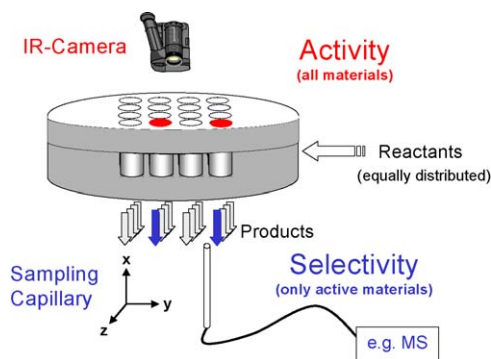


Fig. 1. Schematic illustration of the 192-fold screening system employed for the study of the acetoxylation reaction.

of all the catalysts contained in the reactor, a choice of the most active candidates via infrared with subsequent GC–MS analysis can be performed. The system can be operated at pressures up to 1.2 bar of absolute pressure when the infrared transparent window is mounted, if it is demounted 10 bar of absolute pressure can be obtained. For the current screening the system was operated at 1.2 bar of absolute pressure.

## 2. Workflow for synthesis and testing

As described above the target lead structure of the study were potassium and palladium-based catalyst systems which were subjected to doping with a variety of elements. The synthesis workflow was adapted in a fashion that the base solutions containing the desired elemental compositions were impregnated as solutions of nitrates on a support material (in this case steatite of Ceramtec) and then subjected to thermal treatment under air at 80 °C for 12 h and a thermal treatment under nitrogen atmosphere under a heating ramp of 5 °C/min to intermittent plateaus at 200 °C for 2 h and 400 °C for 4 h. In general all elements were added in a single impregnation step with a total loading of 3 wt.% based on the metals loaded. After fines removal the samples were subjected to the catalytic test in 192-fold test unit with IR and GC–MS analysis at a total sample volume of 0.2 ml. For a detailed description of the test unit and the algorithms used for testing please see Ref. [12]. Quantification of the gas composition was performed by GC–MS, conversion and selectivities are calculated on the basis of butadiene and the respective acetoxylation products 1-acetoxybutadiene (1-ABD) and 1,4-diacetoxybutene (1,4-DAB).

All calculations concerning potential reaction pathways and stabilities of occurring products have been performed with the GAMESS [13] quantum chemistry package on PC type hardware running the operating system GNU/Linux. All structures were fully optimized, the topology of the energy hypersurface for the stationary points have been verified using numeric calculations of the corresponding hessian matrices.

## 3. Test results for the catalyst system Pd–K–Bi

The testing campaigns were initiated by subjecting the catalysts to standard gas mixtures containing butadiene, acetic

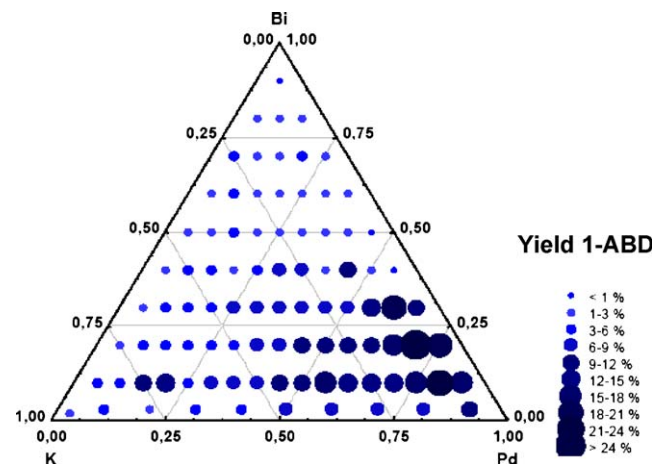


Fig. 2. Performance of samples (expressed as yield of 1-ABD) in the system Pd/K/Bi for a total loading of 2 wt.% at a feed of 1% butadiene, 5% acetic acid, 10% O<sub>2</sub>, balance N<sub>2</sub>, 2000 h<sup>-1</sup>, 180 °C.

acid and oxygen with nitrogen as balance gas at the ratios of (0.5–10%):(1–10%):(1–10%) with nitrogen being the balance for a GHSV of 2000 h<sup>-1</sup>. The typical levels for the experimental design were 0.5, 5 and 10 vol.% for butadiene and 1, 5 and 10 vol.% for oxygen and acetic acid. In the design of experiments a reduced factorial three-level design was used with nine measurement points. Typically the reaction temperature was varied in the range of 180–310 °C with the best results being obtained at lower temperatures.

It is illustrative to start with the scanning of the compositional space of the Pd–K–Bi catalysts. For this purpose catalysts were prepared as described above with a constant metal loading on the carrier and a variation of the constituent molar ratios according to a full coverage algorithm within the ternary. The catalytic test revealed that a pronounced optimum exists for the catalyst composition for high molar ratios of Pd and low molar ratios of Bi and K (see Fig. 2). In Fig. 2 the yields obtained 1-ABD for a feed of 1% butadiene, 5% acetic acid, 10% O<sub>2</sub>, balance N<sub>2</sub>, 2000 h<sup>-1</sup>, 180 °C are plotted. Although not included in the graphs due to the much lower yields: the activity and selectivity patterns for 1,4-DAB follow the patterns for 1-ABD exactly for the Pd–K–Bi system. For the ternary of Pd–K–Sb similar optima are found, nevertheless the maximum yields for 1-ABD and 1,4-DAB that could be obtained for the antimony-based system was slightly lower than for bismuth based catalysts. The finding that the optimum ratios within the ternary catalysts system are in the range of 70% Pd, 20% Bi and 10% K on a molar basis supports the hypothesis that phase formation of phases like Pd<sub>3</sub>X or Pd<sub>4</sub>X as active species may be the reason for the positive catalytic behaviour [14].

Fig. 3a represents a plot of the catalytic effect on butadiene conversion to 1-ABD for the variation of the Pd- and the K-ratios for a constant Bi-molar ratio. It can be seen that increasing K-molar ratios and decreasing Pd-molar ratios have a pronounced effect on the activity of the catalyst which drops sharply already at low levels of the K-molar ratio. It is amazing to see that apart from the very low and high ranges of K-molar ratios the selectivity to the main product 1-ABD (and 1,4-DAB as minor

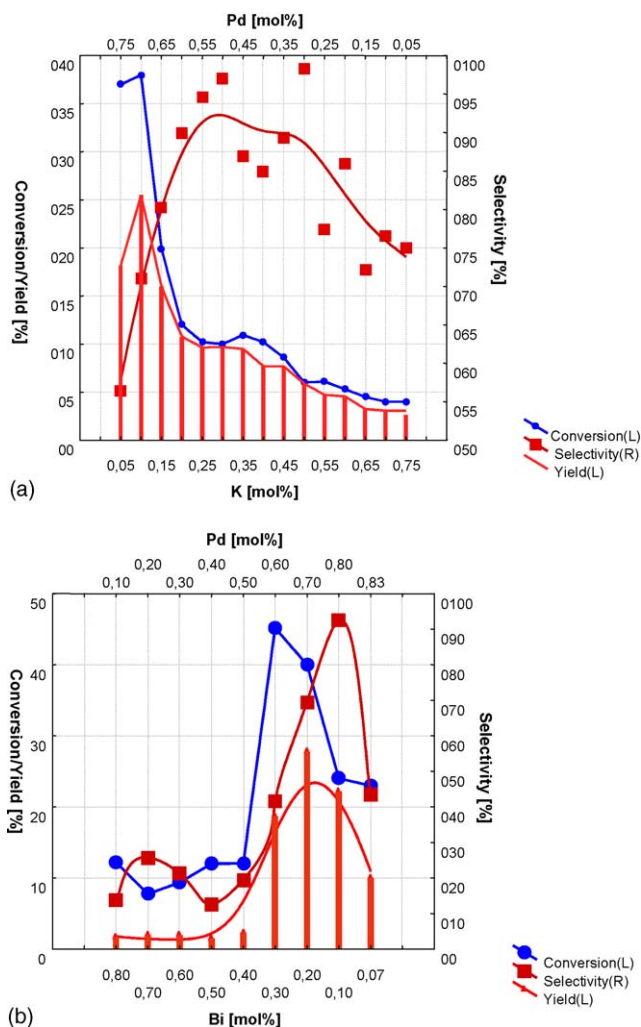


Fig. 3. (a) Performance of the samples (expressed as yield of 1-ABD) in the system Pd/K/Bi visualized as varying Pd- and K-molar ratios with constant Bi-molar ratio of 20% for a total loading of 2 wt.% at a feed of 1% butadiene, 5% acetic acid, 10% O<sub>2</sub>, balance N<sub>2</sub>, 2000 h<sup>-1</sup>, 180 °C. (b) Performance of the samples (expressed as yield of 1-ABD) in the system Pd/K/Bi visualized as varying Pd- and Bi-molar ratios with constant molar ratio of K of 10% for a total loading of 2 wt.% at a feed of 1% butadiene, 5% acetic acid, 10% O<sub>2</sub>, balance N<sub>2</sub>, 2000 h<sup>-1</sup>, 180 °C.

side product which is not illustrated here) stays high and almost at a similar level over a wide range. In combination the highest yields to 1-ABD and 1,4-DAB (not displayed) can be obtained at a molar ratio of K of 10%. This behaviour is totally different for a change in the molar ratio of Bi versus Pd as illustrated in Fig. 3b. In this plot the K-molar ratio was kept constant and the molar ratios of Pd and Bi were varied. Here it can be seen that only for a small range of Pd- and Bi-molar ratios high yields of 1-ABD (and 1,4-DAB, respectively) can be obtained with activity and selectivity of the catalyst candidates dropping sharply outside this range. The maximum conversion level is reached at Bi-levels of 35% molar ratio, a maximum selectivity level is reached at 10% molar ratio. The maximum yield for 1-ABD is reached at a Bi-molar ratio of 20%. As already discussed above, the optimal ranges of the molar ratios for Pd to Bi seem to reflect the formation of defined phases of Pd<sub>x</sub>Bi<sub>y</sub>.

#### 4. Influence of the reaction conditions on the catalyst performance for the system Pd–K–Bi

Both, reaction temperature and feed composition have a pronounced influence on the catalyst performance. Concerning the reaction temperature it was observed that for a feed of 1% butadiene, 5% acetic acid, 10% O<sub>2</sub>, balance N<sub>2</sub>, 2000 h<sup>-1</sup> the maximum selectivity to 1-ABD and 1,4-DAB were obtained at temperatures around 180 °C. The conversion increase beyond 180 °C is coupled to a major decrease in selectivity with a conversion of 30% and 85% selectivity to 1-ABD at 180 °C and a conversion of 60% and a selectivity of 55% 1-ABD at 200 °C. This tendency is seen not only for the optimal catalyst formulation, but also for catalyst formulations outside of the range for optimum yields.

The optimisation of the feed parameters is illustrated for the optimum catalyst molar ratios in the system Pd–K–Bi of Pd<sub>70</sub>K<sub>10</sub>Bi<sub>20</sub> in the Fig. 4a and b. From the figures it can be concluded that optimal yields of 1-ABD and 1,4-DAB (not displayed) can be obtained for low concentrations of the olefin (in this case butadiene) and an excess of acetic acid and oxygen. Interestingly enough for the butadiene to acetic acid ratio, a

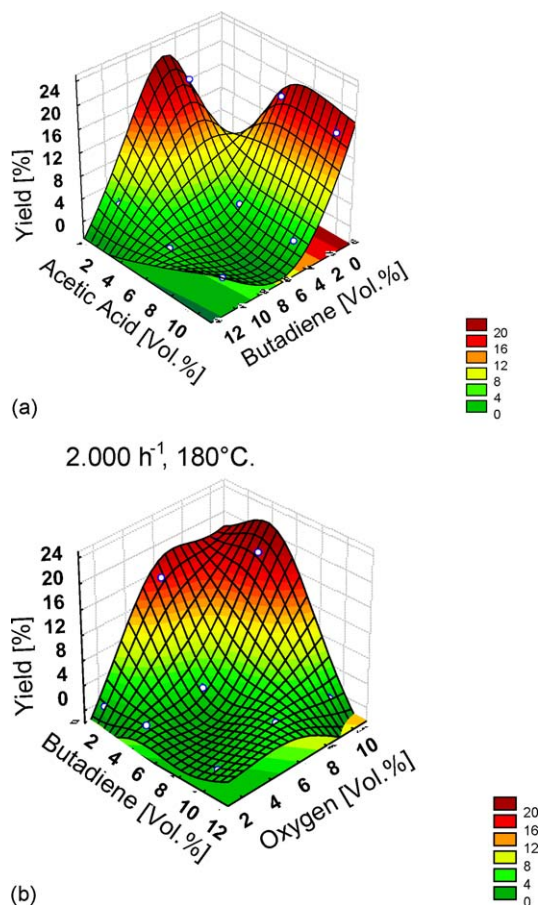


Fig. 4. (a) Performance of the sample Pd<sub>70</sub>K<sub>10</sub>Bi<sub>20</sub> (expressed as yield of 1-ABD) visualized as varying butadiene and acetic acid content at a constant feed of 6% O<sub>2</sub>, balance N<sub>2</sub>, 2000 h<sup>-1</sup>, 180 °C. (b) Performance of the sample Pd<sub>70</sub>K<sub>10</sub>Bi<sub>20</sub> (expressed as yield of 1-ABD) visualized as varying butadiene and oxygen content at a constant feed of 6% acetic acid, balance N<sub>2</sub>, 2000 h<sup>-1</sup>, 180 °C.

second maximum is visible at low acetic acid concentration and intermediate butadiene concentration (see Fig. 4a). For the butadiene to oxygen plot in Fig. 4b no second maximum was observed: clearly oxygen excess and minor concentrations of butadiene. As for the effect of temperature the dependence of the maximum yield on the feed composition is similar throughout all catalyst compositions, even those being outside the optimum molar fractions of Pd–K–Bi.

### 5. Screening of different multinary catalyst compositions

In the first phase of testing a comparison for the different doping elements in the ternary system Pd–K–X was conducted. For this initial library we focussed on the dopants Bi, Sb, Se and Te as semiconductor components. From the open literature it was known that elements capable of forming semiconductor-oxides showed superior performance in the gas phase acetoxylation reaction [14]. Generally in our experimental studies it was found that bismuth containing samples were superior over Te, Se doped catalysts. The highest yields of 1-ABD over bismuth containing

samples were 22%, 1,4-DAB was obtained with a yield of 3% at maximum. For tellurium and selenium doped samples maximum yields for 1-ABD were around 4% and around 1% for 1,4-DAB. Antimony containing samples show comparable results with bismuth containing catalysts, still the overall yields that could be obtained were slightly lower (18% 1-ABD, 3% 1,4-DAB). In a second campaign the alkali component was varied for the catalyst system Pd–X–Bi with X = Na, K, Cs, Ca. The highest yields were obtained for the K based catalysts (see above for maximum yields); for the other elements the following order was found for the maximum yield: Calcium 11% 1-ABD, 3% 1,4-DAB, Cesium 10% 1-ABD, 3% 1,4-DAB and Sodium 8% 1-ABD, 2% 1,4-DAB.

Our next approach for improving the catalyst system was to introduce a fourth component in the catalyst system Pd–K–Bi. In these campaigns the dopants Cu, Ag, Au as candidates also being described for vinylacetate synthesis, Sn and In as additional semiconductor compounds and Rh and Pt as additional platinum metals were explored. In these libraries the K-molar ratio was kept constant at 10% and the three components Pd–Bi–X were mapped as described above in a ternary with a full coverage

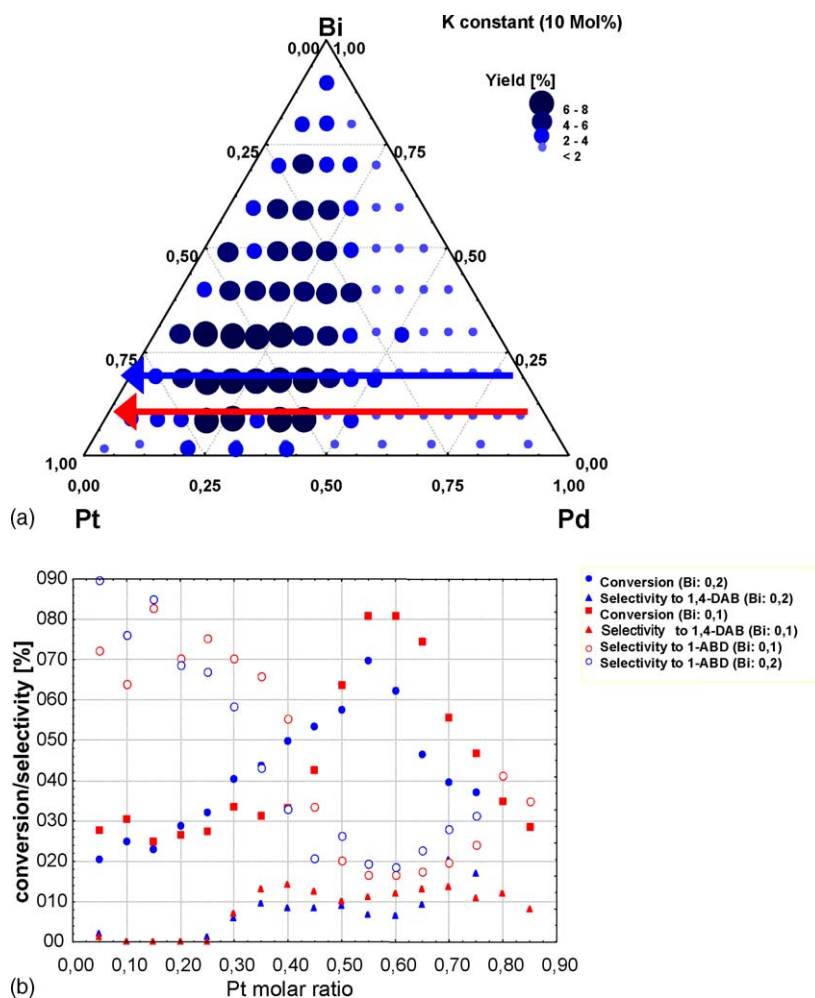


Fig. 5. (a) Performance of samples (expressed as yield of 1,4-DAB) in the system Pd/K/Bi/Pt for a total loading of 2 wt.% at a feed of 1% butadiene, 5% acetic acid, 10% O<sub>2</sub>, balance N<sub>2</sub>, 2000 h<sup>-1</sup>, 180 °C. The two arrows indicate the *iso*-molar ratio lines of Bi for plot (b). (b) Performance of samples (expressed conversion of butadiene and selectivity to 1-ABD and 1,4-DAB as a function of Pt- vs. Pd-content) in the system Pd/K/Bi/Pt for a total loading of 2 wt.% at a feed of 1% butadiene, 5% acetic acid, 10% O<sub>2</sub>, balance N<sub>2</sub>, 2000 h<sup>-1</sup>, 180 °C. K was kept constant at 10% and Bi was kept at 10% and 20%, respectively.



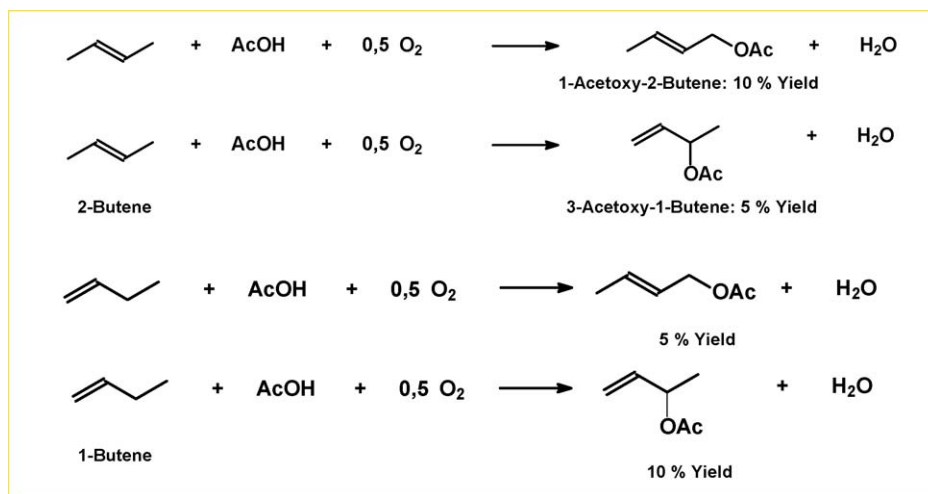


Fig. 6. Products and product amounts obtained for Pd<sub>36</sub>K<sub>10</sub>Bi<sub>45</sub>Pt<sub>9</sub> for a total loading of 2 wt.% at a feed of 1% 1- or 2-butene, 5% acetic acid, 10% O<sub>2</sub>, balance N<sub>2</sub>, 2000 h<sup>-1</sup>, 180 °C.

algorithm. The general observations for all the additional dopants except platinum were similar. In all cases 1-ABD was the main product and a lowering of the maximum yield of 1-ABD and 1,4-DAB with respect to the undoped Pd–K–Bi system was observed. Within the ternary diagrams a broadening of optimum catalyst composition for maximum 1-ABD yield was visible, still the optimum generally remained at the palladium rich end with 45–80 mol% Pd, 5–40% Bi and 5–40% of the additional component (keeping in mind that K was kept constant at 10% for the these experiments and is not calculated in the balance here). The overall tendencies towards the reaction parameters were similar though: high yields of 1-acetoxybutadiene (1-ABD) and 1,4-diacetoxybutene (1,4-DAB) could only be found at low butadiene and high oxygen and acetic acid contents in the feedstream.

The only catalyst system that behaved substantially different to the catalyst candidates mentioned above was the Pd–K–Bi–Pt system. Here the yields for 1-ABD were only lowered to a minor extend (19%) accompanied by a broadening of the optimum catalyst composition in the range as described above. The Pt-doped catalyst system was the only composition in combination with Pd–K–Bi that showed an increase in the 1,4-DAB yield from 4% to 8% of the doped catalyst. Interestingly the higher yields for 1,4-DAB were obtained for Pt-rich samples exclusively with an approximate molar composition of Pd 5–45%, Bi 10–70% and Pt 25–75% (notice that K was kept constant at 10% molar ratio for all samples. Fig. 5a illustrates this shift within the ternary, whereas in Fig. 5b the corresponding conversion/selectivity

behaviour is plotted as a function of the platinum versus palladium content (K was kept constant at 10%, Bi was either at 10% or 20% molar ratio for the respective samples). It can be seen that at low Pt contents high selectivities to 1-ABD are obtained, with rising Pt-content the selectivity to 1-ABD decreases and both selectivity to 1,4-DAB and the degree of conversion rise.

## 6. Pd–K–Bi–X: reactions with other olefins

Of special interest for us was the comparison of the reactivity of the various samples with other olefins. Initial tests were performed with 1- and 2-butene as substrate molecules. For both butenes the acetoxylation products 1-acetoxy-2-butene and 3-acetoxy-2-butene were obtained at moderate yields. The interesting fact in this study was that in both cases the acetoxylation of the butane was always preferred in the allylic position, still the competitive acetoxylation product could be observed (Fig. 6). Other olefins that were employed as substrates for the acetoxylation reaction were ethene and propene. Within the Pd–K–Bi–X libraries the highest yields of acetoxylation products were obtained for samples containing Pt as a dopant.

## 7. Interpretation of the results obtained in the light of theoretical considerations for the mechanism prevalent in the acetoxylation reaction

For the oxidative acetoxylation, two alternative reaction pathways can be considered and will be discussed in the

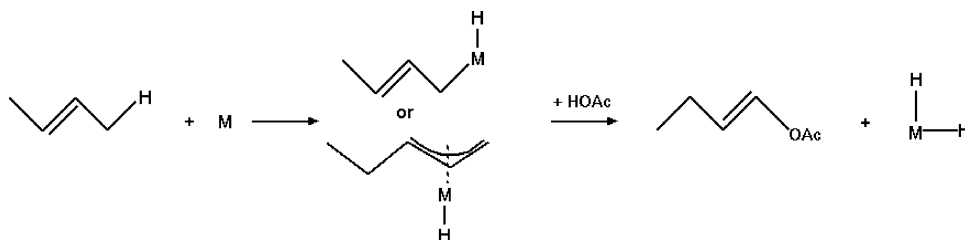


Fig. 7. Hypothetical C–H activation pathway for the acetoxylation reaction of butadiene.

Table 1  
Reaction energies for the hydrogen abstraction from different olefins

Educt/product	Without O <sub>2</sub> (kJ/mol)	With O <sub>2</sub> (kJ/mol)
Ethene → vinyl radical	254.4	134.4
Propene → allyl radical	151.7	31.7
1-Butene → allylic activation	135.9	24
2-Butene → allylic activation	144	15.9
1-Butene → 1-H-abstraction	264.4	144.4
1,3-Butadiene → 1-H-abstraction	260.9	140.9
1,3-Butadiene → 2-H-abstraction	242.3	122.3
Acetic acid → acetoxy radical	238.4	118.4

As baseline for the energy either H<sub>2</sub> or H<sub>2</sub>O are taken. All energies are results of DFT-calculations at the UB3LYP/6-311(p,d) level (without ZPE corrections).

Table 2  
Reaction energies for the reaction olefin + acetic acid → acetoxy compound + -hydrogen

Educt/product	Without O <sub>2</sub> (kJ/mol)	With O <sub>2</sub> (kJ/mol)
Ethene → 1-acetoxyethene	81.8	-159.2
Propene → 1-acetoxypropene	103.6	-137.4
2-Butene → 1-acetoxy-1-butene	84.8	-156.1
2-Butene → 1-acetoxy-2-butene	88.2	-152.8
2-Butene → 2-acetoxy-2-butene	76.6	-164.4
2-Butene → 3-acetoxy-1-butene	90.6	-150.4
1,3-Butadiene → 1-acetoxy-1,3-butadiene	97.4	-143.6
1,3-Butadiene → 2-acetoxy-1,3-butadiene	84.8	-156.2
1,3-Butadiene → 1,4-acetoxy-2-butadiene	60.7	-180.3
1,3-Butadiene → 1,2-acetoxy-2-butadiene	62.5	-178.4
1,3-Butadiene → 1,3-acetoxy-2-butadiene	50.6	-190.4

The energies in the second column take the oxidation of hydrogen to water into account. All energies are results of DFT-calculations at the B3LYP/6-311(p,d) level (without zero point vibrational corrections).

following. The first reaction pathway involves oxidative addition of a low-valent transition metal atom to a C–H  $\sigma$ -bond (see Fig. 7). Such reactions are known to proceed in a facile fashion [15], especially for allylic hydrogen bonds since the resulting modification in the electronic structure of the affected carbon atom can be compensated in the  $\pi$ -system of the allyl group and its mesomeric effect. Bond activation energies for several positions in different olefins are given in Table 1.

This type of C–H activation mechanism seems to be reasonable at least for substrates like propene or butenes possessing allylic hydrogen atoms since it plausibly explains the high selectivity towards allylic substitution. Our DFT

Table 3  
Reaction energies for the addition of an acetoxy radical to an olefin

Educt/product	Reaction energy (kJ/mol)
Ethene → 1-acetoxyethyl radical	-84.2
Propene → 1-acetoxypropyl radical	-84
1-Butene → 1-acetoxy-2-butyl radical	-82.8
2-Butene → 2-acetoxy-3-butyl radical	-88
1,3-Butadiene → 1-acetoxy-2-butadienyl radical	-116
1,3-Butadiene → 3-acetoxy-2-butadienyl radical	-53

All energies are results of DFT-calculations at the UB3LYP/6-311(p,d) level (without ZPE corrections).

calculations indicate, that this mechanism fails to explain our measured product distribution in the case of butenes and 1,3-butadiene as substrate. The preferred products are neither the most stable isomers from a thermodynamic point of view nor have the substituted hydrogen atoms an increased reactivity (Table 2).

Therefore we propose a second different reaction mechanism involving the activation of acetic acid by O–H bond scission in the first step. Assuming that free acetoxy radicals are formed by a formally homolytic cleavage of the O–H bond (which is slightly more facile than cleaving a C(sp<sup>2</sup>)–H bond (see Table 1)) the experimental findings can be explained easily.

Acetoxy radicals are capable to attack the olefinic  $\pi$ -system forming an intermediate product of radical nature (see Table 3). This product can stabilise itself by releasing an H atom (C–H bond scission) and restoring the  $\pi$ -system (see Fig. 8). In the case of 1,3-butadiene as a substrate, the intermediate can react with a second radical or acetic acid molecule to form 1,4-DAB. This mechanism explains the selectivity for allylic substitution because C–H bond cleavage can occur in the *ipso*-position of the acetoxy group as well as in  $\beta$ -position. Furthermore, it can explain the high selectivity for 1-ABD and 1,4-DAB in the product spectrum of 1,3-butadiene as a substrate: As can be seen in Fig. 9, the intermediate product formed by 1-addition is highly favoured, because the radical is stabilised due to delocalisation. Since the transient radicals have a finite lifetime, it becomes obvious, why low partial pressures of the olefin and an excess of acetic acid and oxygen in the feed gas are required for reasonable yields of the desired product in favour of polymeric by-products.

The above proposed mechanism also offers an immediate explanation for the observations of the acetoxylation of 1- and 2-butene: the indistinguishable product spectrum of 1-butene and 2-butene as reaction substrates are most likely caused by fast, transition metal catalysed 1,2 hydrogen shift setting 1-butene and 2-butene into their thermodynamic equilibrium.

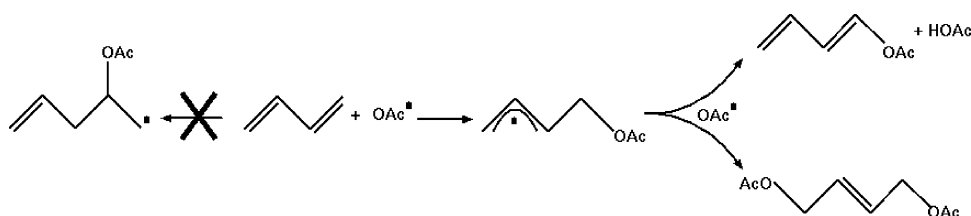


Fig. 8. Reaction of 1,3-butadiene with an acetoxy radical.

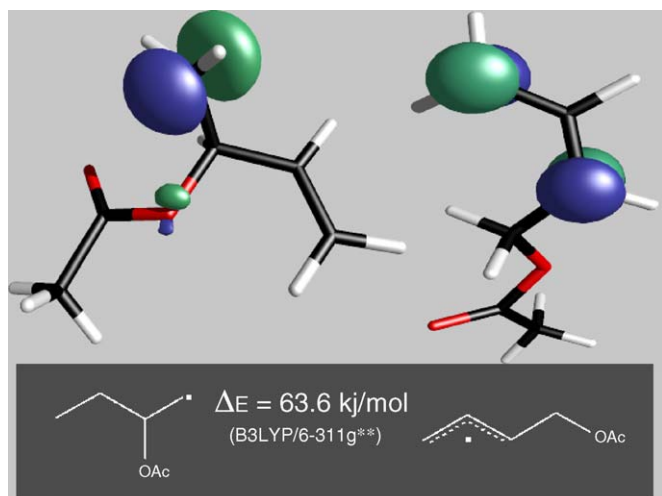


Fig. 9. Relative stability of intermediate radicals for the addition of an acetoxy radical to 1,3-butadiene as result of a DFT calculation. Note that facile rearrangement towards the more stable intermediate is possible.

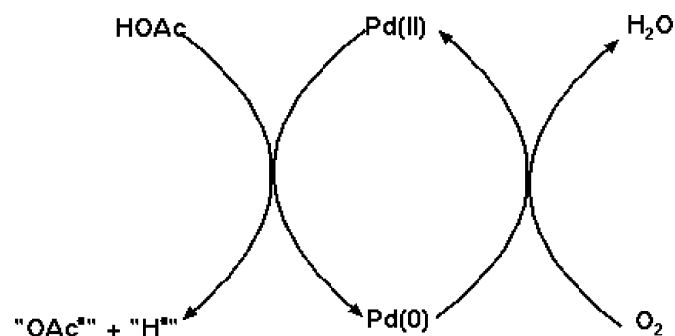


Fig. 10. Redox-cycle of the catalyst in acetoxylation reaction.

As can be derived from our calculated reaction energies, the presence of oxygen is required to make the overall reaction exothermic. A hypothetical oxygen free reaction producing hydrogen as a by-product would be strongly endothermic. We therefore propose that the major role of the catalyst is to activate acetic acid in the way described above. The oxygen in the feed gas serves as re-oxidizing agent for the metal compounds and regenerates the catalyst by removing hydrogen species in the form through reaction to water (see Fig. 10). The promoting role of the platinum in the catalyst system could be attributed to the higher oxidation capability of the platinum species involved.

Our proposed mechanism goes well along the lines of the findings of Neurock et al. [16]. They conclude from their

theoretical studies, that surface oxygen may also facilitate the acetic acid activation in a similar mechanism for the synthesis of vinyl acetate. Here, all adsorbed species are bound in the coordination sphere of surface Pd-atoms without occurrence of free radicals. Also other groups have suggested acetoxylation mechanisms via radical pathways [17,18].

## 8. Conclusions

High throughput experimentation has become an indispensable tool for catalysis research. In this study we tried to illustrate that by combination of computational chemistry and accelerated screening structure property relationships can be derived. The results that we obtained for the gas phase acetoxylation show that the major challenge concerning an economic gas phase diacetoxylation for butadiene process is still unmet: small yields of 1,4-DAB at partial conversions render a gas phase route unattractive. Still the Pd–K–Bi–Pt system shows an improvement in 1,4-DAB yield for the target conversion and seems to be an interesting candidate material also for other related conversions.

## References

- [1] K. Weissermehl, H.-J. Arpe, *Industrielle Organische Chemie*, 5th ed., Wiley-VCH, 1998.
- [2] T. Onoda, US Patent 3,922,300, Mitsubishi Chemical, 1974.
- [3] S.A. Schunk, C. Baltes, J. Klein, *Oil Gas Eur. Mag.* 31 (2005) 77.
- [4] I. Ono, US Patent 3,671,577, Toya Soda Manufacturing Co., Ltd., 1970.
- [5] T. Shizumi, US Patent 3,872,163, Kuraray Co., Ltd., 1972.
- [6] S. Kamiyama, US Patent 4,354,961. Toa Nenryo Kogyo Kabushiki Kaisha, 1980.
- [7] H. Shinohara, *Appl. Catal.* 10 (1984) 27.
- [8] H. Shinohara, *Appl. Catal.* 14 (1985) 145.
- [9] H. Shinohara, *Appl. Catal.* 24 (1986) 17.
- [10] H. Shinohara, *Appl. Catal.* 30 (1987) 203.
- [11] H. Shinohara, *Appl. Catal.* 50 (1989) 119.
- [12] J. Klein, W. Stichert, W. Strehlau, A. Brenner, D. Demuth, S.A. Schunk, H. Hibst, S. Storck, *Catal. Today* 81 (2003) 329.
- [13] M.W. Schmidt, K.K. Baldrige, J.A. Boatz, S.T. Elbert, M.S. Gordon, J.J. Jensen, S. Koseki, N. Matsunaga, K.A. Nguyen, S. Su, T.L. Windus, M. Dupuis, J.A. Montgomery, *J. Comput. Chem.* 14 (1993) 1347–1363.
- [14] T. Komatsu, K. Inaba, T. Uezono, A. Onda, T. Yashima, *Appl. Catal. A* 251 (2003) 315.
- [15] J. March, *Advanced Organic Chemistry*, 4th ed., Wiley, New York, 1992.
- [16] M. Neurock, W.D. Provine, D.A. Dixon, G.W. Couiston, J.J. Lerou, R.A. van Santen, *Chem. Eng. Sci.* 51 (1996) 1691–1699.
- [17] J.M. Davidson, P.C. Mitchell, *Front. Chem. React. Eng.* 1 (1984) 300.
- [18] S. Nakamura, T. Yasui, *J. Catal.* 17 (1971) 315.